NASA Technical Memorandum 100611

THERMAL STRESS IN HIGH TEMPERATURE CYLINDRICAL FASTENERS

Max L. Blosser

MAY 1988

National Aeronautics and Space Administration

Langley Research Center
Hampton, Virginia 23665-5225

THERMAL STRESS IN HIGH TEMPERATURE CYLINDRICAL FASTENERS

Max L. Blosser
NASA Langley Research Center
Hampton, VA 23665

Abstract

Uninsulated structures that are fabricated from carbon or silicon-based structural materials and that are allowed to become hot during flight are attractive for the design of some components of hypersonic vehicles. They have the potential to reduce weight and increase vehicle efficiency. Because of manufacturing constraints, these structures will consist of parts which must be fastened together. The thermal expansion mismatch between conventional metal fasteners and carbon or silicon-based structural materials may make it difficult to design a structural joint which is tight over the operational temperature range without exceeding allowable stress limits. In this study, algebraic, closed-form solutions for calculating the thermal stresses resulting from radial thermal expansion mismatch around a cylindrical fastener are developed. These solutions enable a designer to quickly evaluate many combinations of materials for the fastener and structure. Using the algebraic equations developed in this study, material properties and joint geometry were varied to determine their effect on thermal stresses. Finite element analyses were used to verify that the closed-form solutions derived in this study give the correct thermal stress distribution around a cylindrical fastener and to investigate the effect of some of the simplifying assumptions made in developing the closed-form solutions for thermal stresses.

Introduction

The National Aerospace Plane (NASP) program has generated a renewed interest in research relating to hypersonic vehicles. The severe aerodynamic heating encountered by reusable hypersonic vehicles makes the structural design of such vehicles a challenge. Uninsulated structures, which are allowed to become hot during flight, are attractive for the design of some components of hypersonic vehicles because they have the potential to reduce weight and increase vehicle efficiency. Some hot structures being considered may reach temperatures approaching 3000 °F. Carbon or silicon-based materials will likely be useful for such structures because they are light and retain strength at elevated temperature.

An example of such a hot structure is a carbon-carbon body flap which was studied as a replacement for the insulated aluminum flap on the Shuttle (ref. 1). In addition, NASA Langley Research Center has a current contract ("Development of Oxidation Protected Carbon-Carbon Lightly Loaded Structures" - contract NAS1-18462) which will include the design and fabrication of a carbon-carbon control surface test article for NASP, such as that shown in figure 1. Because of manufacturing constraints, these structures and similar hot structures will consist of smaller pieces which must be fastened together. Ductile metal fasteners are desirable for assembling these multiple pieces. However, the thermal expansion mismatch between the metal fastener and carbon or silicon-based structural materials makes it difficult to design a structural joint which is tight over the operational temperature range without exceeding allowable stress limits.

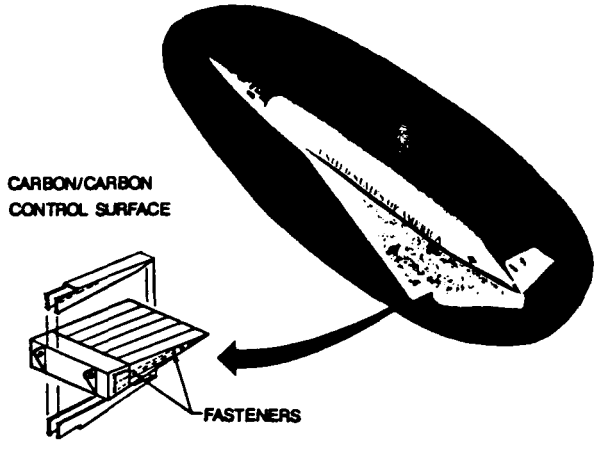

Fig. 1: Hot structures for reusable hypersonic vehicles

The problems encountered using a standard cylindrical fastener in a high temperature joint are illustrated in figure 2. In the figure the fastener is assumed to have a much larger coefficient of thermal expansion (CTE) than the structure. If the fastener is snug in the radial direction at room temperature, high thermal stresses will result at elevated temperature. If sufficient radial clearance is left around the fastener so that it is just snug at elevated temperature, then it may be too loose at room temperature. Similarly, if the fastener is axially snug at room temperature it will be loose at elevated temperature, and it must be prestressed considerably at room temperature to remain snug at elevated temperature. The radial thermal stress or axial prestress required to maintain an acceptably tight joint over the operational temperature range may cause premature failure of the joint. Therefore, a joint

consisting of a standard cylindrical fastener that joins pieces of the selected high temperature material should be analyzed to determine if there are satisfactory combinations of radial clearance and axial prestress at room temperature which will produce acceptable stresses at elevated temperature.

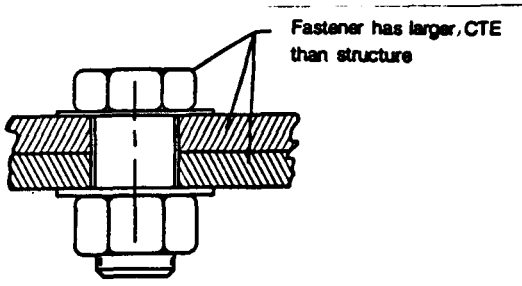

	Joint condition	
	Room temperature	High temperature
Radial direction	Snug Loose	High thermal stresses Snug
Axial direction	Snug Pre-stressed	Loose Snug

Fig. 2: Problem areas for cylindrical fastener joints in high temperature applications

In this paper, simple solutions for calculating the thermal stresses resulting from radial thermal expansion mismatch around a cylindrical fastener are developed to enable a designer to evaluate quickly many combinations of materials. The solutions developed do not address the axial prestress.

Although similar solutions were found in the literature, no explicit solution for the thermal stresses around a cylindrical fastener was found. References 2-4 contain axisymmetric plane-stress solutions, but these solutions do not involve temperature or thermal expansion. References 5-9 contain similar solutions involving thermal expansion, but do not address quite the same problem as this paper. (A more detailed discussion of references 2-9 is given in Appendix A.) Consequently, algebraic equations for the thermal stresses in a finite ring of material around a cylindrical fastener of a different material are developed in this study. Similarly, algebraic equations for the thermal stresses around a hollow cylindrical fastener are also developed. Equations are also presented that account for the effect of an initial clearance between the fastener and surrounding material. The equations developed in this study are used to study the effect of varying joint geometry and material properties on the thermal stresses in a cylindrical fastener joint. Three-dimensional finite element analyses are used to verify these solutions and to evaluate the effect of some of the simplifying assumptions on the magnitude and distribution of the thermal stress.

Symbols

a	radius of fastener
a_i	inside radius of hollow fastener
A,B,C,D	constants defined by boundary conditions
b	radius of structure around fastener
E	modulus of elasticity
L	length
L_o	length at initial temperature
n	integer
P	pressure at interface between fastener and structure
r,θ,z	cylindrical coordinates
T	temperature
T_o	initial temperature
u	displacement
α	coefficient of linear thermal expansion (CTE)
δ	initial clearance around a cylindrical fastener
ϕ	Airy stress function
ε	strain
ν	Poisson's ratio
σ	stress

Subscripts

f	fastener
g	gap
max	maximum
r	r direction
s	structure around the fastener
z	z direction
θ	θ direction

Closed-Form Solutions

The objective of the following analysis is to develop a simple equation to predict the thermal stresses around a cylindrical fastener at elevated temperature. The thermal stresses predicted by this analysis occur because the fastener has greater thermal expansion in the radial direction than the surrounding structure. The fastener is also assumed to have greater thermal expansion in the axial direction than the surrounding structure and, with increasing temperature, will tend to loosen axially, relieving any axial prestress. If appreciable normal stresses develop at the interface between the fastener and structure, friction will inhibit the axial slippage of the fastener and thereby induce out-of-plane stresses in the joint. However, in the present analysis the assumption is made that there is no friction between the fastener and surrounding structure. Thus, no significant stresses are introduced in the thickness direction of the material and a condition of plane stress results. The fastener and surrounding structure are assumed to undergo a uniform temperature change and to expand radially as isotropic materials although the CTE's of the two materials differ. For simplicity, the fastener is assumed to be surrounded by a disk of material with the fastener at the center. In most joints the shape of the structure will be much more complicated, and the thermal stresses will vary somewhat around the fastener. Also, for simplicity the ends of the bolt, including the head, are neglected (see fig. 3). With these assumptions the problem becomes an axisymmetric, plane-stress problem.

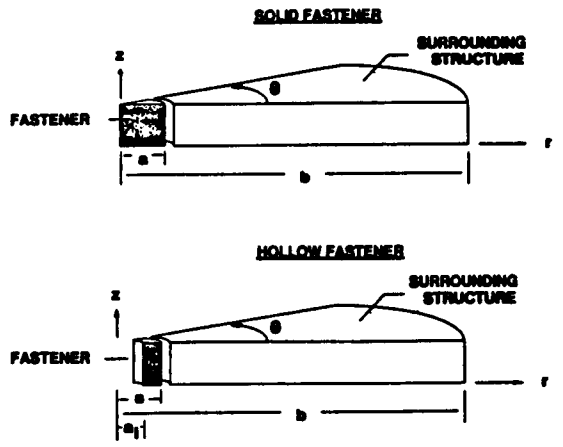

Fig. 3: Idealization of joint geometry

Solid Fastener Solution

The general equations developed in Appendix B (B12 and B13) for axisymmetric stresses and displacements are now used to find the thermal stresses around an idealized cylindrical fastener (fig. 3) at elevated temperature. If the fastener and structure are assumed to be at a uniform temperature and to expand relative to the center of the fastener, the thermal displacement is simply proportional to the radial position. Therefore, by superposition a thermal expansion term is added to equation (B13) for radial displacement to produce:

$$u_r = \frac{1}{E}\left(- \frac{A\,(1+\nu)}{r} + 2\,C\,(1-\nu)\,r \right) + r\,\alpha\,\Delta T \quad (1)$$

The stresses and displacement of the fastener and surrounding material are determined by applying the appropriate boundary conditions. For the fastener:

at $r = a$, $\sigma_{r_f}(a) = -P$

where P is the pressure at the interface between the fastener and structure and

at $r = 0$, $\sigma_{r_f}(0)$ is finite.

Applying these boundary conditions to equations (B12), the constants A and C are found to be:

$$A = 0, \quad \text{and} \quad C = -\frac{P}{2} \quad (2)$$

Therefore, the radial displacement for the fastener is given by:

$$u_{r_f} = -\frac{P\,r}{E}(1-\nu_f) + r\,\alpha_f\,\Delta T \quad (3)$$

Substituting equations (2) into (B12) shows that the fastener is in hydrostatic compression,

$$\sigma_{r_f} = \sigma_{\theta_f} = -P \quad (4)$$

For the structure surrounding the fastener, the boundary conditions are:

at $r = a$, $\sigma_{r_s}(a) = -P$ and at $r = b$, $\sigma_{r_s}(b) = 0$

Applying these boundary conditions to equations (B12), the constants A and C are found to be:

$$A = \frac{P\,b^2}{1 - (\frac{b}{a})^2} \quad \text{and} \quad C = -\frac{P}{2}\left(\frac{1}{1 - (\frac{b}{a})^2}\right) \quad (5)$$

The expression for radial displacement in the structure surrounding the fastener therefore becomes:

$$u_{r_s} = -\frac{P}{E_s}\left(\frac{1}{1 - (\frac{b}{a})^2}\right)\left(\frac{b^2}{r}(1+\nu_s) + (1-\nu_s)r\right) + r\,\alpha_s\,\Delta T \quad (6)$$

Displacement compatibility at the interface between the fastener and structure, $r = a$, requires that the radial displacements be equal at that point. Equations (3) and (6), with $r = a$, can be combined and solved for the interface pressure, P.

$$P = \frac{E_s\left((\frac{b}{a})^2 - 1\right)(\alpha_f - \alpha_s)\,\Delta T}{(\frac{b}{a})^2(1+\nu_s) + (1-\nu_s) + \frac{E_s}{E_f}\left((\frac{b}{a})^2 - 1\right)(1-\nu_f)} \quad (7)$$

The stress distributions in the structure surrounding the fastener can be found by combining equations (B12) and (5) to produce:

$$\sigma_{r_s} = -P\left(\frac{(\frac{b}{r})^2 - 1}{(\frac{b}{a})^2 - 1}\right) \quad (8)$$

$$\sigma_{\theta_s} = P\left(\frac{(\frac{b}{r})^2 + 1}{(\frac{b}{a})^2 - 1}\right) \quad (9)$$

where P is given by equation (7).

Several limiting cases of the solution for thermal stresses around a cylindrical fastener are now considered. These limiting cases give insight into the behavior of the joint and provide simpler expressions for thermal stresses in the joint. If the structure around the fastener is shrunk to an infinitely thin ring, the stresses in the fastener approach zero. The only nonzero stress is the hoop stress in the ring of structure which is given by the simple expression:

$$\sigma_{\theta_s} = E_s\,(\alpha_f - \alpha_s)\,\Delta T \quad (10)$$

If the fastener is surrounded by an infinite sheet ($b/a \to \infty$), equation (7) reduces to the following form:

$$P = \frac{E_s\,(\alpha_f - \alpha_s)\,\Delta T}{(1+\nu_s) + \frac{E_s}{E_f}(1-\nu_f)} \quad (11)$$

and the stresses in the structure around the fastener become:

$$\sigma_{\theta_s} = -\sigma_{r_s} = \left(\frac{a}{r}\right)^2 P \qquad (12)$$

If the fastener material is much stiffer than the surrounding structure ($E_f >> E_s$), then equation (11) reduces to:

$$P = \frac{E_s\,(\alpha_f - \alpha_s)\,\Delta T}{1 + \nu_s} \qquad (13)$$

and the stresses may be found by substituting equation (13) into equations (8) and (9). Similarly, if the surrounding structure is much stiffer than the fastener material ($E_s >> E_f$), then equation (11) reduces to:

$$P = \frac{E_f\,(\alpha_f - \alpha_s)\,\Delta T}{1 - \nu_f} \qquad (14)$$

Hollow Fastener Solution

The solution for thermal stresses of a hollow cylindrical fastener can be found by following a similar procedure. The equations for stresses and displacements in the structure surrounding the fastener will have the same form for the hollow fastener as for the solid fastener, however, the equation for the interface pressure between the fastener and surrounding structure will be different.

The stresses and displacement for the idealized hollow fastener (fig. 3) can be found by applying the following boundary conditions:

at $r = a_i$, $\sigma_r(a_i) = 0$

and at $r = a$, $\sigma_r(a) = -P$

Applying these boundary conditions to equations (B12), the constants A and C are found to be:

$$A = \frac{P\,a^2 a_i^2}{a^2 - a_i^2}, \quad \text{and} \quad C = -\frac{P\,a^2}{2\,(a^2 - a_i^2)} \qquad (15)$$

The expression for radial displacement in the fastener, therefore, becomes:

$$u_{r_f} = -\frac{P}{E_f}\left(\frac{1}{1 - \left(\frac{a_i}{a}\right)^2}\right)\left(\frac{a_i^2}{r}(1+\nu_f) + (1-\nu_f)\,r\right) + r\,\alpha_f\,\Delta T \qquad (16)$$

As in the solid fastener solution, displacement compatibility at the interface between the fastener and surrounding structure, $r = a$, requires that the radial displacements be equal at that point. Equations (6) and (16), with $r = a$, can be combined and solved for the interface pressure P to give:

$$P = \frac{E_s\left[\left(\frac{b}{a}\right)^2 - 1\right](\alpha_f - \alpha_s)\,\Delta T}{\left(\frac{b}{a}\right)^2(1+\nu_s) + (1-\nu_s) + \frac{E_s}{E_f}\left(\frac{b^2 - a^2}{a_i^2 - a^2}\right)\left\{\left(\frac{a_i}{a}\right)^2(1-\nu_f) - (1-\nu_f)\right\}} \qquad (17)$$

The stresses in the structure surrounding the fastener can be found by substituting the value of P from equation (17) into equations (8) and (9). The stress distributions in the hollow fastener can be found by combining equations (B12), and (15) to produce:

$$\sigma_{r_f} = -P\left(\frac{\left(\frac{a_i}{r}\right)^2 - 1}{\left(\frac{a_i}{a}\right)^2 - 1}\right) \qquad (18)$$

$$\sigma_{\theta_f} = P\left(\frac{\left(\frac{a_i}{r}\right)^2 + 1}{\left(\frac{a_i}{a}\right)^2 - 1}\right) \qquad (19)$$

Fastener With Initial Clearance

Fasteners may have an initial clearance at room temperature. Equation (7) may be easily modified to account for an initial clearance. The temperature change which closes the gap due to the initial clearance must be calculated. This temperature can be found by equating the radial position of the expanded fastener and hole. As discussed in reference 10, if the CTE's are assumed to be independent of temperature, the exact expression for thermal expansion can be found by integrating the equation:

$$dL = L\,\alpha\,dT \qquad (20)$$

to produce

$$L = L_o\,e^{\alpha(T - T_o)} \qquad (21)$$

Equating the radial position of the expanded fastener and hole therefore produces:

$$a\,e^{\left(\alpha_f\,\Delta T_g\right)} = (a + \delta)\,e^{\left(\alpha_s\,\Delta T_g\right)} \qquad (22)$$

Solving equation (22) for the temperature change produces:

$$\Delta T_g = \frac{\ln\left(1 + \frac{\delta}{a}\right)}{\alpha_f - \alpha_s} \qquad (23)$$

where δ is the initial clearance. The temperature change calculated using equation (23) can be subtracted from the total temperature change, and the net temperature change can be substituted into equation (7) to find the corresponding thermal stresses. Note, however, that the term ($\Delta T - \Delta T_g$) must be positive.

Finite Element Analyses

The finite element method is commonly used to numerically analyze the stresses in joints. Therefore, finite element solutions were obtained

for comparison with the mathematically derived solutions presented in this study. Finite element analyses were used to verify that the equations derived in this study give the correct thermal stress distribution around a cylindrical fastener. In addition the finite element analyses were used to investigate the effect of friction and the protruding end of the fastener on the thermal stress distribution. An existing, general-purpose finite element program, Engineering Analysis Language (EAL) (ref. 11), was used for the analyses.

A three-dimensional finite element model (see figure 4) was used to represent a solid cylindrical fastener joint configuration. A five-degree wedge-shaped model of the fastener and structure was used as indicated on the figure. Similar models were used to model both a hollow fastener joint and a joint with a fastener which protruded from the structure.

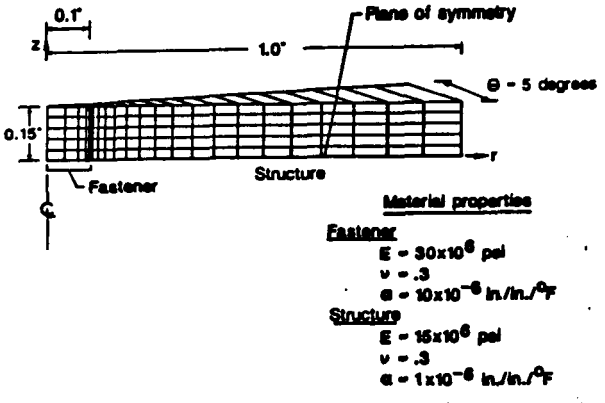

Fig. 4: Finite element model of solid cylindrical fastener and surrounding structure

Particular, but arbitrary, dimensions were chosen for each joint modeled. The radius of the cylindrical fastener was 0.1 inch and the radius of the surrounding structure was 1.0 inch. The thickness of the cylindrical fastener model was 0.15 inch, but the symmetry constraints applied on the lower surface made the model respond as though it were 0.3 inch thick. The inside radius of the hollow fastener was 0.05 inch. For the model of the protruding fastener, the fastener extended 0.1 inch above the structure. An arbitrary set of isotropic stiffness properties was used (see figure 4).

Three-dimensional, six-node and eight-node, linear elements were used to model the fastener and eight-node linear elements were used to model the surrounding structure. The radial dimensions of the elements were varied parabolically to achieve a finer mesh near the interface between the fastener and surrounding structure. The finer mesh near the interface was required for efficient prediction of the expected stress gradients in that region. The resulting finite element mesh can be seen in figure 4. Nodes on the sides and bottom of the model were constrained to remain in their respective planes but were free to move within those planes.

The most challenging portion of the finite element analysis was modeling the contact between the fastener and surrounding material along the bearing surface. Adjacent nodes along this boundary were connected by zero-length elements which had high stiffness perpendicular to the bearing surface and no stiffness tangent to the surface. The elements allowed relative motion along the boundary between the adjacent nodes, but not perpendicular to it. The model was set up so that if one of these elements was found to be in tension, the element stiffness could be reduced to an insignificant value. For the cases analyzed, however, none of the zero length elements was in tension. For the solid fastener, one case was analyzed with the zero length elements having large (essentially infinite) stiffnesses in all degrees of freedom. This case simulated the highest possible stresses due to friction.

Results and Discussion

Comparison of Closed-Form and Finite Element Solutions

The thermal stresses calculated from the closed-form solutions developed in this paper are compared to those calculated from the finite element models previously described. Figure 5 shows the thermal stress comparison for a solid fastener subjected to a 1000 °F temperature increase. The radial and hoop stresses are shown as a function of radial position for both the fastener and structure. The shaded region of the figure represents the fastener, and the unshaded region represents the surrounding structure. Stresses calculated using the three-dimensional finite element model are indicated by symbols, and the plane-stress solution stresses are indicated by solid lines. The results show excellent agreement for both the magnitude and distribution of thermal stresses. The peak stress of approximately 80,000 psi is indicative of the large thermal stresses which may occur in hot structures with cylindrical fasteners. The peak stresses in the structure occur at the interface between the fastener and structure. The magnitude of the compressive radial stress is slightly less than the magnitude of the tensile hoop stress.

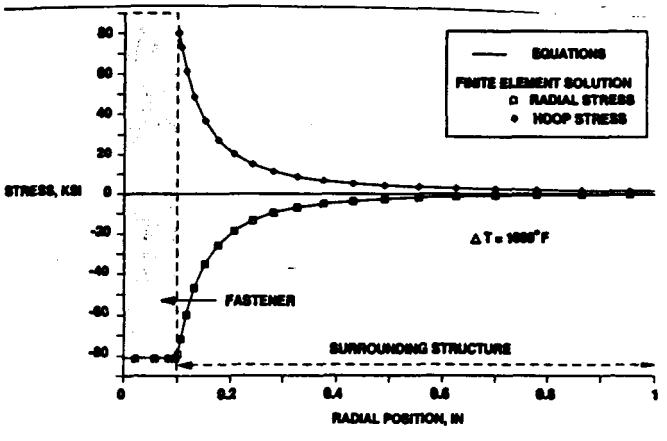

Fig. 5: Thermal stresses for solid cylindrical fastener

The fastener is in hydrostatic compression with stress equal to the peak radial stress in the structure, as shown by the constant hoop and radial stresses in the fastener. Because the structural hoop and radial stresses are tensile and compressive respectively, the von Mises stress in the structure will be considerably larger than in the fastener. The geometry and loading are axisymmetric, so the in-plane shear stress is inherently zero. The plane-stress solution neglects the z stress and out-of-plane shear stresses. In the absence of friction between the fastener and structure, the three-dimensional finite element analysis also predicts negligible out-of-plane stresses for the relatively thick model analyzed.

Figure 6 shows a similar comparison of thermal stresses for a hollow fastener. The geometry, material properties, and loading are the same as for figure 5, except that the fastener is hollow. The shaded band represents the wall of the hollow fastener. Again, the only significant stresses are the radial and hoop stresses in the fastener and structure. The figure shows the excellent agreement between the three-dimensional finite-element and plane-stress solutions. The stress distribution in the structure is similar to that for the solid fastener, however, the magnitudes of the stresses are lower. The stress distribution in the hollow fastener is completely different than in the solid fastener. The radial stress goes to zero on the inner surface of the fastener, as expected. The hoop stress in the hollow fastener is much larger than that in the solid fastener. The peak hoop stress occurs on the inner surface of the hollow fastener, and for this example, is more than double the stress in a solid fastener. Again, the out-of-plane stresses predicted by the three-dimensional finite element solution were negligible.

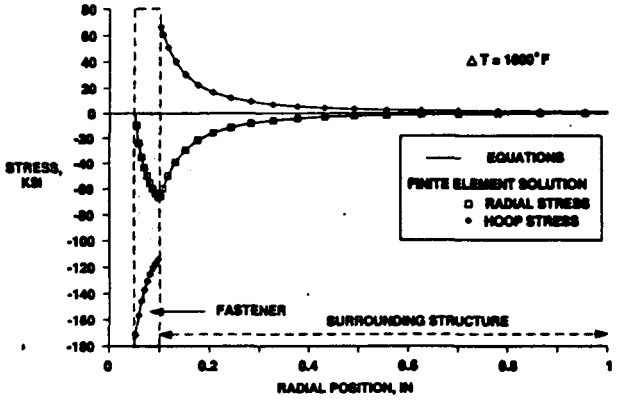

Fig. 6: Thermal stresses for hollow fastener

Effects of Geometry and Material Properties on Thermal Stress

The equations for thermal stress around a solid cylindrical fastener were used to determine the effect of varying material properties and geometry. Figure 7 shows the maximum thermal

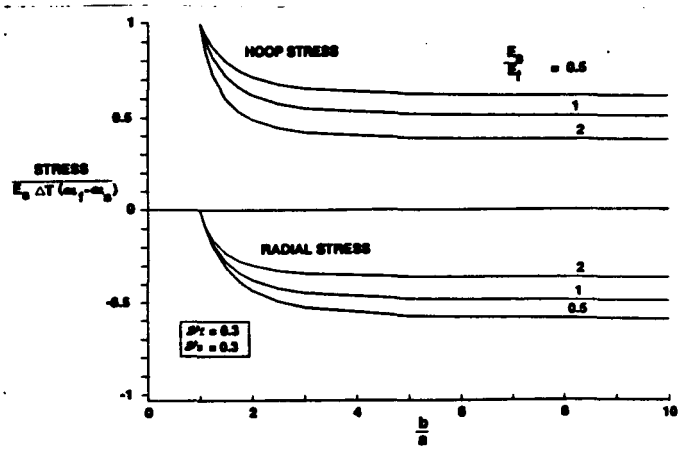

Fig. 7: Maximum structural thermal stresses for solid fastener as a function of ratio of structure-to-fastener radius

stresses in the structure around a solid fastener as a function of the ratio of the structure radius a to the fastener radius b . The thermal stress is nondimensionalized by dividing by an expression that represents the maximum possible thermal stress in the structure. The ratio of structural modulus to fastener modulus is varied to produce a set of curves on the figure. The ratio b/a was varied between one and ten. For b/a > 5, the maximum stresses become almost insensitive to further changes in b/a and the simpler equations (11) and (12) can be used to calculate thermal stresses. As b/a approaches unity, the structure becomes a thin ring around the fastener and the radial stresses approach zero. The ring of material cannot restrain the greater thermal expansion of the fastener, and almost all of the thermal expansion mismatch is accommodated by hoop strain in the ring. The non-dimensional hoop stress therefore approaches unity (see eqn. (10)). When the modulus of the structure is greater than that of the fastener, more of the thermal expansion mismatch is accommodated by strain in the fastener, and the nondimensional stress in the structure is reduced. Conversely, if the modulus of the structure is less than that of the fastener, the nondimensional stress in the structure is increased.

The Poisson's ratios of the fastener and structure were also varied to determine their effect on thermal stress. In figure 8 the maximum thermal stress (hoop stress at r=a) in a solid fastener in an infinite sheet of structure is shown as a function of Poisson's ratio of the fastener. The Poisson's ratio of the structure is also varied to produce a set of curves. The values of Poisson's ratio are varied from zero to 0.5, the range possible with isotropic materials. Increasing the fastener Poisson's ratio effectively stiffens the fastener, which is in two-dimensional hydrostatic compression, and thereby increases the peak thermal stress. Increasing the structure Poisson's ratio, however, decreases peak thermal stresses.

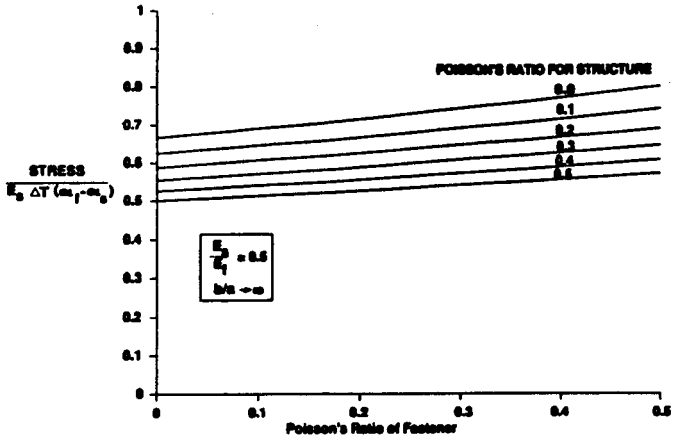

Fig. 8: The effect of Poisson's ratio on solid fastener maximum thermal stress

Figure 9 shows a comparison of the maximum thermal stresses of a hollow fastener to those of a solid fastener with similar geometry, material properties, and loading. The ratio of hollow-to-solid fastener stresses is shown as a function of the ratio of the hollow fastener inner-to-outer radius. The figure shows that even a small hole in the center of a fastener increases the stress in the fastener by a factor of 2. The stress increase occurs because the stress distribution is changed by the introduction of the hole. On the inner surface of the fastener the radial stress must go to zero so that the fastener cannot be in hydrostatic compression. The hoop stress increases significantly, compared to a solid fastener. As the wall of the hollow fastener becomes thinner, the stress in the structure is reduced, but the fastener stress remains high. When the fastener modulus is greater than that of the structure, the fastener stress ratio increases as the fastener wall is made thinner. When the moduli are equal, the fastener stress ratio remains constant with wall thickness. When the structural modulus is greater, the fastener stress ratio decreases as the fastener wall is made thinner. For a specified wall thickness, a stiffer fastener modulus produces a lower stress ratio.

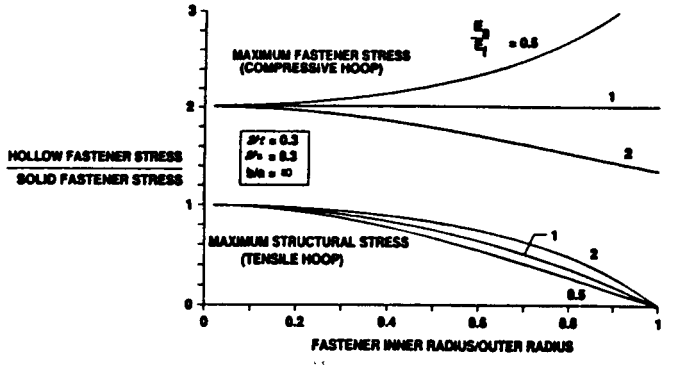

Fig. 9: Thermal stresses in hollow fastener compared to those in a solid fastener

Fastener Protrusion Beyond Surrounding Structure

Most fasteners extend through the structure being fastened. However, to develop the algebraic equations in this study, the fastener was assumed not to protrude beyond the surrounding structure. A finite element model was used to investigate the effects of this assumption by calculating the thermal stresses for a particular fastener which protrudes beyond the structure. Figure 10 shows the distribution of radial stress in such a joint. Away from the fastener the stresses are uniform through the thickness, which is consistent with the plane-stress solution. Near the fastener the stresses in the structure increase slightly toward the protruding end of the fastener, compared to the stresses in a joint in which the fastener does not protrude. The portion of the fastener protruding beyond the structure is free to thermally expand radially, but the portion of the fastener within the structure is constrained by the surrounding structure. Thus, the fastener expands more near the protruding end of the fastener than towards the center of the structure. The presence of a fastener head would therefore be expected to increase the local, peak thermal stresses in the structure even more than a protruding fastener shank. The peak stresses for a joint with a protruding fastener are shown in Table 1, along with the stresses predicted using the plane-stress solution developed in this study. The peak radial stress in the structure is about 15 percent higher for the protruding fastener. However, these higher stresses are localized at the fastener/structure interface at the free surface and for many materials may be alleviated by local yielding. Significant out-of-plane stresses, not present in the plane-stress solution, were calculated for the joint with a protruding fastener. However, these out-of-plane stresses are low compared to the in-plane stresses. If brittle materials or materials with low out-of-plane strengths are used in the joint, a more detailed analysis of the joint may be required.

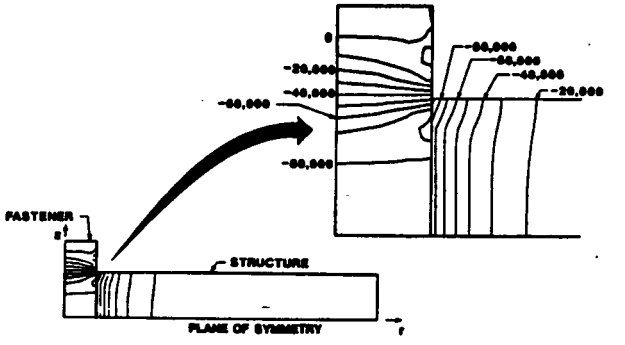

Fig. 10: Radial thermal stress distribution (psi) for solid fastener protruding beyond structure

Type of Stress	Idealized Joint	Protruding Fastener	Friction (no slippage)
Fastener			
Radial	-81,000	-62,000	-139,000
Hoop	-81,000	-84,000	-139,000
	0	-23,000	-154,000
r-z Shear	0	14,000	-69,000
Structure			
Radial	-81,000	-84,000	-161,000
Hoop	81,000	85,000	149,000
z	0	8,000	89,000
r-z Shear	0	3,000	-71,000

Table 1: Maximum calculated thermal stresses (psi)

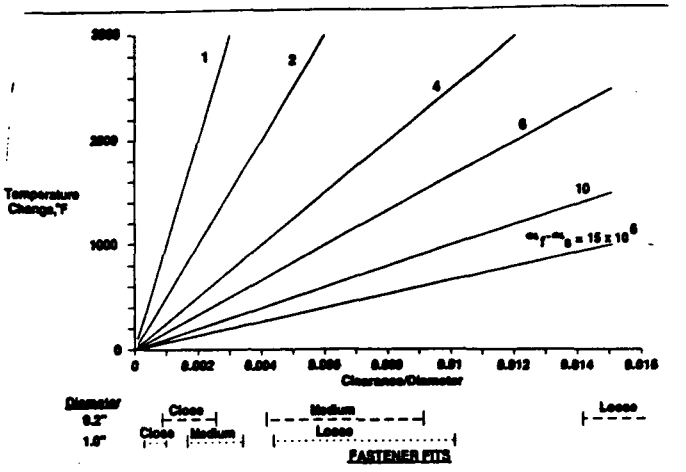

Fig. 11: Temperature change required to close initial clearance

Friction Between Fastener and Structure

Finite element analysis was also used to investigate the maximum possible thermal stresses due to friction. The adjacent nodes on the boundary between the structure and fastener were forced to remain together. The maximum stresses calculated for the joint are shown in Table 1. The peak stresses for the worst case friction are almost double the stresses calculated assuming no friction. The largest shear stresses occur along the interface between the fastener and structure. The shear stresses increase linearly along the length of the interface and reach a maximum near the free surface. In an actual joint some slipping will likely occur along the interface to alleviate some of the frictional stresses. This finite element analysis and the plane-stress solution represent the upper and lower bounds, respectively, of the thermal stresses for this particular idealized joint. The large difference in stresses indicates that friction can have a significant effect. Therefore, further investigation may be necessary to determine the effect of friction on the thermal stresses around a cylindrical fastener. A designer might also consider taking steps to reduce friction in a joint, such as using a high temperature lubricant.

Fastener With an Initial Clearance

The temperature change required to close an initial clearance around a cylindrical fastener is shown as a function of clearance to diameter ratio in figure 11. A family of curves is shown for various differences in thermal expansion coefficients between fastener and structure. As expected, for larger differences in thermal expansion coefficients, smaller increases in temperature will close the initial clearance. Table 2, from reference 12, lists the clearances for several categories of fits. On figure 11, the ranges for close-sliding fit, medium running fit, and loose running fit are indicated for fasteners with 0.2 and 1.0 inch diameters. For a given type of fit, a smaller diameter fastener will require a larger temperature increase to close the initial clearance. Consequently, for a given type of sliding or running fit, a larger fastener will tend to have higher thermal stresses than a

Diameter Range, in.		Clearance (Thousands of an inch on diameter)					
Over	To	Close Fit		Medium Fit		Loose Fit	
		min.	max.	min.	max.	min.	max.
0.04	0.12	0.1	0.45	0.6	1.4	2.5	5.1
0.12	0.24	0.15	0.5	0.8	1.8	2.8	5.8
0.24	0.40	0.2	0.6	1.0	2.2	3.0	6.6
0.40	0.71	0.25	0.75	1.2	2.6	3.5	7.0
0.71	1.19	0.3	0.95	1.6	3.2	4.5	10.0
1.19	1.97	0.4	1.1	2.0	4.0	5.0	11.5
1.97	3.15	0.4	1.2	2.5	4.9	6.0	13.5
3.15	4.73	0.5	1.5	3.0	5.5	7.0	15.5
4.73	7.09	0.6	1.8	3.5	6.7	8.0	18.0
7.09	9.85	0.6	2.0	4.0	7.5	10.0	21.5

Table 2: Limits of clearance for running and sliding fits from ref. 12

smaller fastener. The effect of an initial clearance can be seen by considering the sample joint analyzed previously in this study, with geometry and material properties defined in figure 4. For a 1000 °F temperature increase, the thermal stresses around a fastener with a close-sliding fit will be reduced by between eight and 28 percent compared to a fastener with no initial clearance. For a medium fit the thermal stress reduction would be reduced by between 44 and 100 percent, and for a loose fit there would be no thermal stress. For the same conditions with one inch diameter fastener, the thermal stresses for the close fit would be reduced by between three and 11 percent; the stresses for the medium fit would reduced by between 18 and 36 percent; and the stresses for the loose fit would be reduced by between 50 and 100 percent.

Concluding Remarks

Algebraic equations derived from closed-form solutions of elasticity equations are presented for thermal stresses in solid and hollow

cylindrical fasteners. The fastener was idealized as a pin surrounded by an annulus of structural material so that an axisymmetric plane-stress solution could be developed. Friction between the fastener and structure was neglected. For these assumptions, excellent agreement was obtained between the thermal stresses predicted by the algebraic equations and by a three-dimensional finite element analysis.

An equation was also developed to predict the temperature required to close an initial clearance around a fastener. This temperature can be subtracted from the total temperature change to calculate the thermal stress of a fastener with an initial clearance at room temperature. For a sample joint the initial fastener fit is shown to have a significant effect on the thermal stresses.

Using the algebraic equations developed in this study, material properties and joint geometry were varied to determine their effect on thermal stresses. The effect of varying the radius of the structure surrounding the fastener was determined. When the ratio of structure to fastener radius exceeds five or six the peak stresses become insensitive to further increases in the ratio. The effect of varying the structure-to-fastener modulus ratio was also shown. Increasing fastener modulus increases thermal stresses in the joint. Thermal stresses of similar hollow and solid fasteners were compared. Hollowing out a fastener increases fastener stresses and decreases structural stresses. The effects of varying the Poisson's ratios of both the fastener and structure are also shown. Increasing the fastener Poisson's ratio effectively stiffens the fastener, which is in two-dimensional hydrostatic compression, and thereby increases the peak thermal stress. Increasing the structure Poisson's ratio, however, decreases peak thermal stresses.

Finite element analysis was used to bound the effects of friction on thermal stresses and to show the effects of a fastener protruding beyond the surround structure. Friction is shown to have the potential to significantly increase the thermal stresses in a joint compared to the stresses calculated neglecting friction. The fastener protruding beyond the surrounding structure is shown to produce slightly higher localized stresses and to introduce relatively low out-of-plane stresses for a particular example.

The equations developed in this paper are intended to provide a designer with a quick, initial estimate of the thermal stresses in and around a cylindrical fastener at elevated temperature. The equations should be used with a good understanding of the assumptions and limitations which went into their derivation.

Appendix A

Literature Review

The problem of calculating thermal stresses around a cylindrical fastener can be reduced to an axisymmetric, plane-stress problem if both the fastener and surrounding material are linearly elastic and isotropic. A general solution for such problems is presented by Little in reference 2 and by Timoshenko and Goodier in reference 3.

A similar problem is solved by Muskhelishvili in reference 4. In this problem an elastic circular disk is inserted into a smaller radius hole in an infinite plate. This solution only gives the normal stress at the boundary between the materials and does not account for a finite annulus around the disk. Also, the solution does not involve the thermal expansion of the two materials.

Several solutions for thermal stresses in the vicinity of cylindrical inclusions were found in the literature. References 5 and 6 present thermal stress solutions for an infinite cylinder imbedded in an elastic medium with different stiffness properties and thermal expansion coefficient in the presence of thermal gradients. The plane-strain solution for a uniform temperature change is presented in reference 5. When converted to a plane-stress solution the equations in reference 5 agree with the present solution for a cylinder with an infinite radius of material surrounding the cylinder. Similarly, the solution in reference 6, when simplified for a constant temperature change and converted to plane stress, also agrees with the current solution and that of reference 5 for a cylinder with an infinite radius of material surrounding the cylinder. The solutions in references 5 and 6, however, do not account for a finite radius of material surrounding the cylindrical inclusion. In references 7 and 8 a plane-stress solution for thermal stresses in a disk with a central shaft is given. The central shaft, however, is rigid and does not expand with temperature. A solution for thermal stresses in a circular plate with a central hot spot is also presented in reference 8. Reference 9 a more complicated problem with a pair of circular inclusions and a nonuniform temperature distribution.

Although the general solution and similar solutions were found in the literature, no explicit solution for the thermal stresses around a cylindrical fastener was found. Consequently, algebraic equations for the stresses in a finite ring of material around a cylindrical fastener of a different material were developed in this study.

Appendix B

General Solution For Axisymmetric Plane Stress

The general plane-stress solution for axisymmetric problems, as outlined in references 2 and 3, is shown in the following mathematical development. The biharmonic equation which defines the Airy stress function for axisymmetric plane stress is:

$$\frac{d^4\phi}{dr^4} + \frac{2}{r}\frac{d^3\phi}{dr^3} - \frac{1}{r^2}\frac{d^2\phi}{dr^2} + \frac{1}{r^3}\frac{d\phi}{dr} = 0 \qquad \text{(B1)}$$

Equation (B1) has a solution in terms of integer powers of r:

$$\phi = r^n \qquad \text{(B2)}$$

Substituting equation (B2) into equation (B1) produces a characteristic equation which leads to the general solution

$$\phi = A \ln(r) + B r^2 \ln(r) + C r^2 + D \qquad (B3)$$

In polar coordinates, the stresses in terms of the Airy stress function are

$$\sigma_r = \frac{1}{r}\frac{\partial \phi}{\partial r} + \frac{1}{r^2}\frac{\partial^2 \phi}{\partial \theta^2}$$

$$\sigma_\theta = \frac{\partial^2 \phi}{\partial r^2} \qquad (B4)$$

$$\sigma_{r\theta} = -\frac{\partial}{\partial r}\left(\frac{1}{r}\frac{\partial \phi}{\partial \theta}\right)$$

Therefore, by substituting the expression for ϕ into equations (B4), the stresses for an axisymmetric problem are found to be

$$\sigma_r = \frac{A}{r^2} + 2B\ln(r) + B + 2C$$

$$\sigma_\theta = -\frac{A}{r^2} + 2B\ln(r) + 3B + 2C \qquad (B5)$$

$$\sigma_{r\theta} = 0$$

In polar coordinates, the definitions of strain are given by

$$\varepsilon_r = \frac{\partial u_r}{\partial r}$$

$$\varepsilon_\theta = \frac{u_r}{r} + \frac{1}{r}\frac{\partial u_\theta}{\partial \theta} \qquad (B6)$$

$$\varepsilon_{r\theta} = \frac{1}{2}\left(\frac{\partial u_\theta}{\partial r} - \frac{u_\theta}{r} + \frac{1}{r}\frac{\partial u_r}{\partial \theta}\right)$$

Hooke's stress-strain relations for an isotropic material in plane stress are

$$\varepsilon_r = \frac{1}{E}\left(\sigma_{rr} - \nu\,\sigma_{\theta\theta}\right)$$

$$\varepsilon_\theta = \frac{1}{E}\left(\sigma_{\theta\theta} - \nu\,\sigma_{rr}\right) \qquad (B7)$$

$$\varepsilon_{r\theta} = \frac{1+\nu}{E}\,\sigma_{r\theta}$$

The displacements may be calculated from the stresses by combining equations (B5), (B6), and (B7) and solving for radial displacement. First solve for the strains to obtain:

$$\varepsilon_r = \frac{\partial u_r}{\partial r} = \frac{1}{E}\left(\frac{A(1+\nu)}{r^2} + 2C(1-\nu)\right.$$

$$\left. + B(1-\nu)[2\ln(r) + 1] - 2\nu B\right) \qquad (B8)$$

$$\varepsilon_\theta = \frac{u_r}{r} = \frac{1}{E}\left(-\frac{A(1+\nu)}{r^2} + 2C(1-\nu)\right.$$

$$\left. + B(1-\nu)[2\ln(r) + 1] - 2B\right) \qquad (B9)$$

Solution of equations (B8) and (B9) produces two expression for radial displacement which must be consistent. They are

$$u_r = \frac{1}{E}\left(-\frac{A(1+\nu)}{r} + 2C(1-\nu)\,r\right.$$

$$\left. + B(1-\nu)[2r\ln(r) - r] - 2\nu B r + \text{const}\right) \qquad (B10)$$

$$u_r = \frac{1}{E}\left(-\frac{A(1+\nu)}{r} + 2C(1-\nu)\,r\right.$$

$$\left. + B(1-\nu)[2r\ln(r) + r] + 2Br\right) \qquad (B11)$$

For equations (B10) and (B11) to be consistent the constant B and the constant in equation (B10) must be zero. The general expressions for plane stress are therefore:

$$\sigma_r = \frac{A}{r^2} + 2C$$

$$\sigma_\theta = -\frac{A}{r^2} + 2C \qquad (B12)$$

and the radial displacement is given by:

$$u_r = \frac{1}{E}\left(-\frac{A(1+\nu)}{r} + 2C(1-\nu)\,r\right) \qquad (B13)$$

The constants A and C can be obtained by substitution of boundary conditions into equations (B12) and (B13).

Acknowledgment

This work is based on the author's Master's thesis. It will be submitted to the faculty of George Washington University. The thesis advisor is Dr. Ahmed K. Noor.

References

1. Blosser, Max L.: Design Studies Of Carbon-Carbon Shuttle Body Flap. NASA CP 2315, pp. 595-612, December 1983.

2. Little, Robert W.: Elasticity. Prentice-Hall, Inc., Englewood Cliffs, New Jersey, 1973.

3. Timoshenko, S.; and Goodier, J. N.: Theory of Elasticity. McGraw-Hill Book Company, Inc., New York, New York, 1951.

4. Muskhelvishvili, N. I.: Some Basic Problems of the Mathematical Theory of Elasticity. P. Noordhoff Ltd, Groningen - The Netherlands, 1963, 4th ed. (1954).

5. Dunders, J.; and Zienkiewicz, O. C.: Stresses Around Circular Inclusions Due to Thermal Gradients with Particular Reference to Reinforced Concrete. Journal of American Concrete Institute, 1964.

6. Tauchert, T. R.: Thermal Stress Concentrations in the Vicinity of Cylindrical Inclusions. Journal of Composite Materials, Vol. 3, January 1969.

7. Thermal-Structural Analysis Manual. Technical Report No. WADD-TR-60-517, vol. I, August 1962.

8. Astronautic Structures Manual, Volume III. NASA TM X-73307, August 1975.

9. Shioya, S.; and Tsuruno, S.: Thermal Stresses in an Infinite Plate with a Pair of Circular Inclusions Under Steady-State Temperature. Journal of Thermal Stresses, September 1986.

10. Blosser, M. L.; and McWithey, R. R.: Theoretical Basis for Design of Thermal-Stress-Free Fasteners. NASA TP 2226, December 1983.

11. Whetstone, W. D.: EISI-EAL Engineering Analysis Language Reference Manual, System Level 312. Engineering Information Services, Inc., San Jose, California, August 1985.

12. Mark's Mechanical Engineers' Handbook. McGraw-Hill Book Company, New York, 1958.

Standard Bibliographic Page

1. Report No.	2. Government Accession No.	3. Recipient's Catalog No.
NASA TM-100611		

4. Title and Subtitle	5. Report Date
Thermal Stress in High Temperature Cylindrical Fasteners	May 1988
	6. Performing Organization Code
7. Author(s)	8. Performing Organization Report No.
Max L. Blosser	
9. Performing Organization Name and Address	10. Work Unit No.
NASA Langley Research Center Hampton, VA 23665-5225	506-43-31-04
	11. Contract or Grant No.
12. Sponsoring Agency Name and Address	13. Type of Report and Period Covered
National Aeronautics and Space Administration Washington, DC 20546-0001	Technical Memorandum
	14. Sponsoring Agency Code

15. Supplementary Notes

This paper was presented at the 29th SDM Conference, April 18-22, 1988, Williamsburg, VA.

16. Abstract

Uninsulated structures that are fabricated from carbon or silicon-based structural materials and that are allowed to become hot during flight are attractive for the design of some components of hypersonic vehicles. They have the potential to reduce weight and increase vehicle efficientcy. Because of manufacturing constraints, these structures will consist of parts which must be fastened together. The thermal expansion mismatch between conventional metal fasteners and carbon or silicon-based structural materials may make it difficult to design a structural joint which is tight over the operational temperature range without exceeeding allowable stress limits. In this study, algebraic, closed-form solutions for calculating the thermal stresses resulting from radial thermal expansion mismatch around a cylindrical fastener are developed. These solutions enable a designer to quickly evaluate many combinations of materials for the fastener and structure. Using the algebraic equations developed in this study, material properties and joint geometry were varied to determine their effect on thermal stresses. Finite element analyses were used to verify that the closed-form solutions derived in this study give the correct thermal stress distribution around a cylindrical fastener and to investigate the effect of some of the simplifying assumptions made in developing the closed-form solutions for thermal stresses.

17. Key Words (Suggested by Authors(s))	18. Distribution Statement
Thermal Stresses High Temperature Fasteners Cylindrical Fasteners	Unclassified - Unlimited Subject Category 39

19. Security Classif.(of this report)	20. Security Classif.(of this page)	21. No. of Pages	22. Price
Unclassified	Unclassified	12	A02

For sale by the National Technical Information Service, Springfield, Virginia 22161